Ligand-Induced Changes in the Conformational Dynamics of a Bacterial Cytotoxic Endonuclease†

Ewald T. J. van den Bremer,‡ Anthony H. Keeble,§ Antonie J. W. G. Visser,|| Arie van Hoek,|| Colin Kleanthous,§ Albert J. R. Heck,‡ and Wim Jiskoot*,⊥

Department of Biomolecular Mass Spectrometry, Bijvoet Center for Biomolecular Research and Utrecht Institute for Pharmaceutical Sciences, Utrecht University, Sorbonnelaan 16, 3584 CA Utrecht, The Netherlands, Department of Biology, University of York, York YO10 5YW, United Kingdom, MicroSpectroscopy Centre, Laboratories of Biochemistry and Biophysics, Wageningen University, Dreijenlaan 3, 6703 HA Wageningen, The Netherlands, and Department of Pharmaceutics, Utrecht Institute for Pharmaceutical Sciences, Utrecht University, Sorbonnelaan 16, 3584 CA Utrecht, The Netherlands

Received January 9, 2004; Revised Manuscript Received February 18, 2004

ABSTRACT: Knowledge about the conformational dynamics of a protein is key to understanding its biochemical and biophysical properties. In the present work we investigated the dynamic properties of the enzymatic domain of DNase colicins via time-resolved fluorescence and anisotropy decay analysis in combination with steady-state acrylamide quenching experiments. The dynamic properties of the apoenzyme were compared to those of the E9 DNase ligated to the transition metal ion Zn^{2+} and the natural inhibitor Im9. We further investigated the contributions of each of the two tryptophans within the E9 DNase (Trp22 and Trp58) using two single-tryptophan mutants (E9 W22F and E9 W58F). Wild-type E9 DNase, E9 W22F, and E9 W58F, as well as Im9, showed multiple lifetime decays. The time-resolved and steady-state fluorescence results indicated that complexation of E9 DNase with Zn^{2+} induces compaction of the E9 DNase structure, accompanied by immobilization of Trp22 along with a reduced solvent accessibility for both tryptophans. Im9 binding resulted in immobilization of Trp22 along with a decrease in the longest lifetime component. In contrast, Trp58 experienced less restriction on complexation of E9 DNase with Im9 and showed an increase in the longest lifetime component. Furthermore, the results point out that the Im9-induced changes in the conformational dynamics of E9 DNase are predominant and occur independently of the Zn^{2+}-induced conformational effects.

Colicins are a group of plasmid-encoded toxins produced by *Escherichia coli* under times of nutrient stress and are used to kill related bacterial cells (*1*). Cell death is generally mediated by one of two types of cytotoxic activity: proton-motive force depolarization by formation of a pore within the innermembrane or a nuclease activity acting within the cytoplasm (*1*). Members of the E-colicin DNase subgroup (E2, E7, E8, and E9) kill the target cell by degrading the chromosomal DNA using a Mg^{2+}-dependent and essentially nonspecific DNase activity (*2*, *3*). The cytotoxic activity is housed within a 134-residue C-terminal domain, with a central domain responsible for binding to the extracellular receptor for vitamin B_{12}, BtuB, and an N-terminal domain required for translocation across the outer membrane of a sensitive bacterial cell (*4*, *5*). An antidote protein, called an immunity protein, is coexpressed to protect the producing cell from the cytotoxic effect of the colicin. These 9−10 kDa proteins bind the DNase domain at an exosite adjacent to the active site (Figure 1). Modeling studies indicated that inhibition relies on the polymeric nature of the DNA and occurs through steric and electronic blocking of binding away from the cleavable bond (*6*). This mode of inhibition is

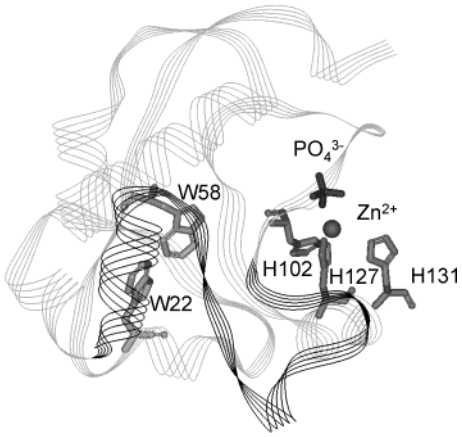

FIGURE 1: Ribbon diagram of the E9 DNase domain showing the Im9 binding site (labeled in black) and the positions of the two tryptophans (W22 and W58) relative to the transition metal and the three coordinating histidine residues plus the ligating phosphate ion.

† The present work was supported by The Netherlands Organization for Scientific Research (NWO 98034 to E.T.J.v.d.B.). C.K. acknowledges support from the BBSRC.

* Corresponding author. Tel: +31(0) 30-2536970. Fax: +31(0) 30-2517839. E-mail: W.jiskoot@pharm.uu.nl.

‡ Department of Biomolecular Mass Spectrometry, Bijvoet Center for Biomolecular Research and Utrecht Institute for Pharmaceutical Sciences, Utrecht University.

§ University of York.

|| Wageningen University.

⊥ Department of Pharmaceutics, Utrecht Institute for Pharmaceutical Sciences, Utrecht University.

10.1021/bi049929c CCC: $27.50
Published on Web 03/19/2004

distinctly different from the conventional mode of nuclease inhibitor binding, e.g., barnase−barstar where the inhibitor directly ligates the active site residues (*7*). Exosite binding by immunity proteins is instead a reflection of the requirement for the DNase to be able to evolve novel immunity protein binding specificities to gain a competitive advantage, with the exosite being the most sequence-divergent region among the four colicin DNase domains (*8*). The active site comprises the C-terminal ~30 residues and contains the consensus sequence for the H−N−H group of homing endonucleases and has a fold conserved with the $\beta\beta\alpha$-Me family of nucleases (*9*, *10*) including the eukaryotic apoptotic DNase CAD (*3*, *11*). The structure of the active site resembles that of a zinc finger. Indeed, transition metals, including zinc, have previously been shown to bind to all colicin DNases (*12*). Ligation of the tetrahedrally coordinated metal ion (Figure 1) involves three histidine residues (His102, His127, and His131) and a noncovalently bound phosphate ion (*6*, *13*).

The immunity protein and metal ions, such as Zn^{2+}, bind with high affinity (femtomolar and nanomolar, respectively) to the colicin DNases, particularly E9, and the binding properties have been extensively studied using a range of biochemical and biophysical techniques (*12*, *14*−*16*). Moreover, ligand binding involves mechanisms that include conformational changes. Ligand-induced conformational changes may be reported by the two tryptophans (W22 and W58; Figure 1), although they are distant from either ligand binding site (*12*, *15*). Furthermore, high-field NMR (*17*, *18*) and (nano) ESI-MS[1] (*19*) have shown that the native state of the E9 DNase is a dynamic population of open and closed conformations. We recently showed this to be true for E2, E7, and E8 colicin DNases as well (*20*). It has been suggested that many conformational changes may be occurring independently of one another (*12*, *19*, *21*). For example, although binding of the Zn^{2+} ion and immunity protein both affects the fluorescence of E9 DNase, the kinetics of immunity protein association (as well the observed fluorescence changes coupled to binding) and dissociation are unaltered by the presence of transition metals in the active site (*12*). This observation overturned a previous hypothesis by Pommer et al. (*16*) that loss of the transition metal is important for cellular uptake of E9 colicin. Specifically, the acceleration of immunity protein dissociation by loss of the bound transition metal was proposed to explain the large difference between the kinetics of immunity protein dissociation ($\sim 10^{-6}$ s^{-1}) and colicin-mediated cell killing ($\sim 10^{-3}$ s^{-1}) (*16*). These observations are congruent with the transition metal induced conformational changes being localized to the active site (*21*, *22*). Nevertheless, it remained unclear how the tryptophan fluorescence was being affected, since both tryptophans are located at a distance from the ligand binding sites (for example, in the X-ray structure the tryptophans are 15 (W22) and 13 Å (W58) from the transition metal binding site), without involving long-range, allosteric, conformational changes.

To gain a better understanding of the molecular origins and the complexity of the conformational changes that occur within colicin DNases, we investigated the interaction of the DNase protein with Zn^{2+}, and its cognate immunity protein, using time-resolved fluorescence spectroscopy and steady-state fluorescence quenching studies. The advantage over other techniques is that processes taking place on the fluorescence time scale (i.e., nanoseconds) can be probed, for example, rotation of the entire protein or segments thereof and interactions with other molecules. We have previously determined the lifetimes and anisotropies of wild-type DNases E2, E7, E8, and E9 without Zn^{2+} and immunity protein (*20*; E. T. J. van den Bremer and A. J. R. Heck, unpublished observations). To probe the effects of Zn^{2+} and immunity protein binding to colicin DNases, we concentrated on the E9 DNase since it is the best characterized colicin DNase. A complicating factor in the analysis of time-resolved fluorescence data of colicin DNases is that the two tryptophans (W22 and W58) are located at a distance <5 Å from each other (in the E9 DNase X-ray structure), which is close enough for energy transfer to occur (*12*). Therefore, single-tryptophan mutants were constructed for E9 DNase, i.e., W58F (W22+) and W22F (W58+), enabling us to study the local environment of the individual tryptophans in the absence of any complicating energy transfer processes.

EXPERIMENTAL PROCEDURES

Protein Samples. Tryptophan-to-alanine mutants were generated as previously described by Keeble et al. (*12*). Wild type and single-tryptophan mutants of the E9 DNases, W22+ (which contains the W58F mutation), and W58+ (which contains the W22F mutation) were purified as described previously (*23*). Im9 was purified as described by Wallis et al. (*15*). Protein concentrations were determined by measuring the UV absorption at 280 nm. Molar absorption coefficients of the E9 wild type, E9 mutants, and Im9 are 17550, 10700 (for both mutants), and 11400 M^{-1} cm^{-1}, respectively. For the metal-loaded proteins, zinc acetate (Merck, Darmstadt, Germany) was used without further purification. Samples contained 10 μM E9 DNase in 50 mM ammonium acetate (pH 7.4) with and without equimolar concentrations of zinc acetate and/or Im9. For measurements of the E9−Zn^{2+}−Im9 complex, Zn^{2+} and Im9 were successively added. For studying the effect of phosphate on the fluorescence characteristics of E9 DNase, 50 mM sodium phosphate buffer (pH 7.4) was used. The samples were prepared at least 24 h prior to analysis.

Picosecond Polarized Time-Resolved Fluorescence and Anisotropy. Time-resolved fluorescence and anisotropy decay times were measured in a home-built setup with mode-locked continuous wave laser excitation and time-correlated photon counting detection. The pump laser was a CW diode-pumped, frequency-doubled Nd:YVO_4. The mode-locked laser was a titanium:sapphire laser coupled with a pulse picker, which decreased the repetition rate of the excitation pulses to 3.8 $\times$ 10^6 pulses per second. The maximum pulse energy was a few picojoules, the wavelength 295 nm, and the pulse duration 3 ps. The temperature was controlled and set at 20 °C. Fused silica cuvettes of 10 mm light path were used. The fluorescence emission was collected at 348.8 nm at an angle of 90° with respect to the direction of the excitation

[1] Abbreviations: E9 DNase, endonuclease domain of colicin E9; Im9, immunity protein for colicin E9 DNase; ESI-MS, electrospray ionization mass spectrometry; NMR, nuclear magnetic resonance; W22+, a tryptophan-to-phenylalanine mutant of the E9 DNase (W22F) that contains only Trp22; W58+, a tryptophan-to-phenylalanine mutant of the E9 DNase (W58F) that contains only Trp58.

light beam. Care was taken to avoid artifacts from depolarization effects. At the front of the sample housing a Glan-laser polarizer was mounted, optimizing the already vertical polarization of the input light beam. Between sample and photomultiplier a single fast lens, an interference filter, a computer-controlled rotatable sheet-type polarizer, and a second single fast lens were placed, focusing the fluorescence on the photomultiplier cathode. All polarizers were carefully aligned, and the setup was finally checked by measuring reference samples. Detection electronics were standard time-correlated single photon counting modules. With a small portion of the mode-locked light a fast PIN photodiode was excited. The output pulses were fed to one channel of a quad constant fraction discriminator and then used as a stop signal for a time-to-amplitude converter. Subsequently, the output pulses were analyzed by an analogue-to-digital converter and were collected in 4096 channels of a multichannel analyzer. The channel time spacing was 11.1 ps. A microchannel plate photomultiplier was used for detection of the fluorescence photons. By reducing the energy of the excitation pulses with neutral density filters, the rate of fluorescence photons was decreased to 30000 per second to prevent pileup distortion (*24*). Other instrumental sources of data distortion were minimized to below the noise level of normal photon statistics (*25*).

Experimental data consisted of repeating sequences of measurements of the polarized emission (parallel and perpendicular component) fluorescence decays of the reference compound (three cycles of 20 s), the protein sample (ten cycles of 20 s), the background (two cycles of 20 s), and again the reference compound. In that way an eventual temporal shift can be traced and corrected. All cuvettes were carefully cleaned and checked for background luminescence prior to the measurements. For obtaining a dynamic instrumental response of the setup, the single-exponential fluorescence decay was measured of *p*-terphenyl in a mixture of cyclohexane and CCl_4 in a 50/50 (%) volume ratio.

Time-Resolved Fluorescence Data Analysis. The time-resolved fluorescence emission $I(t)$ and anisotropy $r(t)$ decays were globally analyzed using a home-built computer program, which employs a reweighed iterative reconvolution method (*26*, *27*). The parameters of the fluorescence decay were obtained from iterative convolution of the measured decay of the reference compound using a modified model function. The experimental data for the fluorescence decay were analyzed on the assumption that it is multiexponential and, thus, can be described by

$$I(t) = \sum_{i=1}^{M} \alpha_i e^{-t/\tau_i} \quad (1)$$

where the relative amplitudes, α_i, and the decay fluorescence lifetimes, τ_i, are the numerical parameters of the ith component to be determined and M is the number of fluorescent components. The weighted average fluorescence lifetime $\langle\tau\rangle$ was calculated according to the equation:

$$\langle\tau\rangle = \sum_{i=1}^{M} \alpha_i \tau_i / \sum_{i=1}^{M} \alpha_i \quad (2)$$

The anisotropy decay can also be described by a sum of M discrete exponential terms:

$$r(t) = \sum_{i=1}^{M} \beta_i e^{-t/\varphi_i} \quad (3)$$

where φ_i is the rotational correlation time of rotational component i and the preexponential term β_i is the contribution of the correlation time of the ith component to the total anisotropy decay.

Fitting sessions were performed by generated starting values of the parameters. The goodness of fit was judged by the value of parameter reduced χ^2 and inspection of the residual function graphs for each data set fitted. For all of our tabulated data (Tables 1−5), reduced χ^2 values were close to unity, and the weighted residuals and autocorrelation function of the residuals were uniformly distributed around zero, indicating an optimal fit. In all cases the simplest model was chosen. Attempted fits of the experimental data to a model with less independent components showed a substantial increase in χ^2 value. On the other hand, an exponential fit using more components did not lead to a significant improvement in χ^2 value.

The angular displacement ψ (in degrees) of the fluorophore was calculated from

$$\frac{\beta_2}{\beta_1 + \beta_2} = {}^1/_2 \cos\psi(\cos\psi + 1) \quad (4)$$

where β_1 and β_2 are the contributions of the correlation times (φ_1 and φ_2) to the total anisotropy decay (*28*).

Steady-State Fluorescence. Steady-state fluorescence experiments were performed on a Fluorolog-3 spectrofluorometer (Jobin Yvon/Horiba, Longjumeau, France) using 1 cm quartz cuvettes. The temperature was controlled and set at 20 °C. Excitation and emission bandwidths were set at 5 nm. For acrylamide quenching experiments, aliquots of acrylamide (1.4 M in ammonium acetate) were added to the protein solution in a range from 0 to 0.33 M. To avoid interference by acrylamide absorption, the excitation wavelength was set to 300 nm. The fluorescence intensity was monitored at 345 nm and corrected for dilution and buffer background.

Stern−Volmer quenching constants (K_{SV}) were obtained from the relationship (*29*):

$$F_0/F = 1 + K_{SV}[Q] = 1 + k_q\langle\tau\rangle[Q] \quad (5)$$

where F_0 and F are the fluorescence intensities in the absence and presence of quencher, respectively, [Q] is the acrylamide concentration, and K_{SV} is the Stern−Volmer quenching constant. In addition, K_{SV} is equal to $k_q\langle\tau\rangle$, where k_q is the apparent bimolecular rate constant for collisional encounters and $\langle\tau\rangle$ is the average excited-state lifetime in the absence of quencher, as determined by time-resolved fluorescence measurements (see above, eq 2).

RESULTS

Fluorescence Decays of Colicin E9 DNase Wild Type and Im9. Typical fluorescence decay curves, with associated fits, are shown in Figure 2 for Im9 and apo-E9 DNase with further results summarized in Table 1. These results illustrate

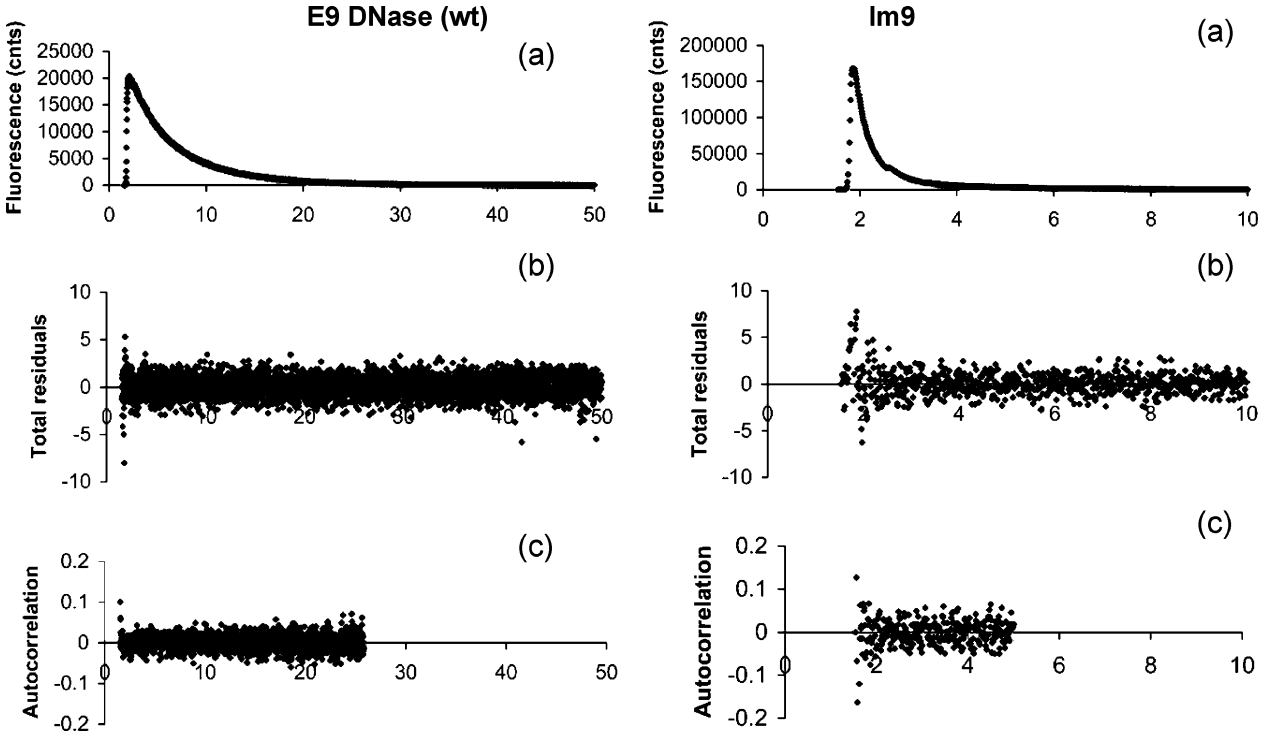

FIGURE 2: Experimental and fitted fluorescence decay of apo-E9 DNase wild type and immunity protein Im9: (a) fluorescence decay, (b) residuals between measured and fitted data, and (c) autocorrelation of the residuals. Fitting parameters are shown in Table 1.

Table 1: Fluorescence Decay Parameters for the E9 DNase Wild Type

protein[a]	α_1[b]	α_2	α_3	α_4	τ_1 (ns)	τ_2 (ns)	τ_3 (ns)	τ_4 (ns)	$\langle\tau\rangle$ (ns)	χ^2[c]
E9		0.135	0.403	0.463		0.45 ± 0.02	2.75 ± 0.04	6.50 ± 0.02	4.17	1.14
E9−Zn^{2+}		0.134	0.438	0.428		0.40 ± 0.02	2.59 ± 0.03	5.89 ± 0.01	3.71	1.16
E9−Im9	0.074	0.375	0.165	0.385	0.03 ± 0.01	0.27 ± 0.01	2.82 ± 0.05	6.71 ± 0.01	3.15	1.08
E9−Zn^{2+}−Im9	0.414	0.0568	0.224	0.305	0.28 ± 0.01	1.52 ± 0.46	3.90 ± 0.40	6.78 ± 0.09	3.13	1.39
E9−PO_4^{3-}		0.134	0.394	0.473		0.43 ± 0.02	2.75 ± 0.03	6.35 ± 0.01	4.14	1.09
E9−Zn^{2+}−PO_4^{3-}		0.122	0.441	0.436		0.48 ± 0.03	2.61 ± 0.03	5.88 ± 0.01	3.78	1.18
Im9	0.604	0.355	0.033	0.086	0.113 ± 0.001	0.39 ± 0.01	2.33 ± 0.03	6.53 ± 0.05	0.34	1.77

[a] E9 and Im9 represent the wild-type E9 DNase and immunity protein Im9, respectively, in the absence and presence of zinc (Zn^{2+}) or phosphate (PO_4^{3-}). [b] α_1, α_2, α_3, and α_4 are the fractional preexponential factors corresponding to lifetimes τ_1, τ_2, τ_3, and τ_4, respectively. [c] Reduced χ^2 values indicate goodness of fit.

how different the environments of the tryptophans are within these two proteins. The decay for the free E9 DNase could be described as a sum of three single-exponential decays with an average lifetime of 4.2 ns. The addition of Zn^{2+} resulted in a decrease of the average lifetime to 3.7 ns. This indicates that at least one of the two tryptophans was quenched. X-ray structures have revealed that the Zn^{2+} ion is tetrahedrally coordinated (*6*). The fourth ligand (in addition to the three histidines) is a single phosphate ion. The phosphate ion binds specifically in the presence of Zn^{2+} with a K_d in the micromolar range (E. T. J. van den Bremer, A. H. Keeble, and A. J. R. Heck, unpublished results) but is not essential to stabilize the Zn^{2+} ion. Therefore, we were interested in measuring the E9 DNase lifetimes with and without Zn^{2+} in the presence of phosphate ions. Table 1 shows that in both cases the lifetimes in phosphate buffer (50 mM sodium phosphate, pH 7.4) are identical to those measured in 50 mM ammonium acetate solutions at identical pH. This demonstrates that the presence of phosphate ions and, most probably, phosphate ion ligation did not change the local environment of both tryptophans.

Prior to lifetime analysis of the E9−Im9 binary complex, lifetimes of the free Im9 protein were determined, showing an ultrashort average lifetime of 0.34 ns. Im9 contains one tryptophan (Trp74), which showed a lifetime decay with four components (see Table 1). The lifetime analysis of the E9−Im9 complex resulted in the appearance of a fourth, ultrashort lifetime component and a reduction of the average lifetime, as compared to the free E9 DNase. Since the observed decay results are from contributions of three tryptophans, it seems impossible to correlate these findings with conformational changes in E9 resulting from interactions with Im9. However, by comparing the lifetime decays of E9−Im9 ($\langle\tau\rangle$ = 3.15 ns) and E9−Zn^{2+}−Im9 ($\langle\tau\rangle$ = 3.13 ns), we conclude that Zn^{2+} binding to the binary complex did not alter the average lifetime.

Time-Resolved Fluorescence Anisotropy of Colicin E9 DNase Wild Type. Time-resolved fluorescence anisotropy measurements were done to gain insight into the conformational dynamics of E9 DNase. Rotational correlation times were recovered from the obtained polarized decays (Table 2). The anisotropy decay curve for free E9 DNase revealed two rotational correlation times (ϕ). The slow motion (ϕ = 8.6 ns) reflects the tumbling of the entire protein while the fast motion (ϕ = 0.27 ns) reflects local mobility of the tryptophans and possibly contributions from energy transfer.

Table 2: Anisotropy Decay Parameters for the E9 DNase Wild Type

protein[a]	β_1[b]	β_2	ϕ_1 (ns)	ϕ_2 (ns)	χ^2[c]
E9	0.071	0.102	0.27 ± 0.02	8.6 ± 0.2	1.14
E9−Zn^{2+}	0.058	0.106	0.26 ± 0.02	8.1 ± 0.1	1.09
E9−Im9	0.088	0.092	0.42 ± 0.02	14.0 ± 0.3	1.12
E9−Zn^{2+}−Im9	0.111	0.102	0.28 ± 0.01	13.4 ± 0.3	1.34
E9−PO_4^{3-}	0.073	0.101	0.24 ± 0.02	9.10 ± 0.20	1.04
E9−Zn^{2+}−PO_4^{3-}	0.066	0.107	0.25 ± 0.16	9.06 ± 0.02	1.09
Im9		0.219		2.69 ± 0.03	3.51

[a] E9 and Im9 represent the wild-type E9 DNase and immunity protein Im9, respectively, in the absence and presence of zinc (Zn^{2+}) or phosphate (PO_4^{3-}). [b] β_1 and β_2 are the amplitudes corresponding to the rotational correlation times ϕ_1 and ϕ_2, respectively. [c] Reduced χ^2 values indicate goodness of fit.

Upon Zn^{2+} binding both motions were mostly unaffected. The presence of phosphate ions had no significant influence on the correlation times (Table 2) and was therefore not further investigated. Ligation of Im9 resulted in a significant increase of the long rotational correlation time from ~8 to ~14 ns. Since the mass of the E9−Im9 complex is significantly larger than that of E9 by itself (24.6 vs 15 kDa), this was expected. The individual Im9 protein showed one rotational correlation time (2.7 ns), reflecting the global motion of the Im9 molecule and indicating that the sole Trp74 is immobile.

Fluorescence Decays of Colicin E9 DNase Mutants W22+ and W58+. The above experiments on the E9−Im9 and E9−Zn^{2+}−Im9 complexes are complicated by the presence of three tryptophans with two less than 5 Å apart. The use of mutant proteins containing less tryptophans than wild type (by mutation to phenylalanine) has previously been shown to be a useful tool to perform fluorescence-based conformational analysis of proteins (*30*−*32*). Two single-tryptophan mutants (W22+ and W58+) were produced (*12*) to probe the effects of ligand binding on the individual tryptophans of the E9 DNase. We have previously demonstrated that electrospray ionization mass spectrometry (ESI-MS) is a sensitive method to measure the conformational state of E9 DNase (*19*). When such experiments were repeated on the two single-tryptophan mutants, W22+ and W58+, they yielded results similar to that of the wild-type E9 DNase, indicating that the mutations had a negligible effect on the structure and stability of the proteins (data not shown).

The results of the fluorescence lifetime analysis of these mutants are summarized in Table 3. The fluorescence decay of the W22+ mutant was adequately described by a sum of three exponential terms (Table 3). The average lifetime of the E9 DNase W22+ mutant decreased after addition of Zn^{2+} (from 3.8 to 2.9 ns). This indicates an increase in collisional quenching of Trp22 by neighboring amino acid residues upon Zn^{2+} binding. Ligating Im9 to the W22+ mutant also resulted in a decrease in the average lifetime, as seen for the E9 DNase wild type. A slight further quench was achieved for the E9−Zn^{2+}−Im9 ternary complex. The free W58+ mutant showed a multiexponential fluorescence decay that could be best described as a sum of four individual components (Table 3). In the absence of Zn^{2+} an ultrashort lifetime of 23 ps with a significant fractional contribution was observed. Upon Zn^{2+} binding the ultrashort component disappeared. Consequently, and also because of an increased contribution (α_4) of the longest individual lifetime (τ_4), the average lifetime was substantially prolonged from 3.6 to 6.5 ns. Remarkably, binding Im9 to apo-W58+ mutant did not result in a significant change in the average lifetime. This is most likely due to the occurrence of changes that largely counteracted one another: the second lifetime (τ_2) *shortened* while the fourth lifetime (τ_4) *lengthened*; furthermore, the corresponding fractional contributions (α_2 and α_4) increased at the expense of α_3.

Comparison of the two binary complexes (DNase−Zn^{2+} and DNase−Im9) with the ternary complex, both for W22+ and the W58+ mutant, demonstrates that the effects induced by Im9 binding overwhelmed those caused by Zn^{2+} binding (Table 3). Nevertheless, the data shown in Table 3 suggest that the fluorescence decays of W22+−Im9 and W22+−Zn^{2+}−Im9 are significantly different. This was confirmed by global analysis of both data sets: when the individual lifetimes of W22+−Im9 and W22+−Zn^{2+}−Im9 were forced to be the same, the overall χ^2 increased to 10.5. When lifetimes were not linked, a χ^2 of 1.17 was observed. Hence, binding of Zn^{2+} to the E9 DNase−Im9 complex does affect the local environment of Trp22, whereas Trp58 is not measurably affected.

Anisotropy Decay Analysis of the W22+ and W58+ Mutant E9 DNases. Both tryptophans have two distinct rotational correlation times (see Table 4). For both mutants, the long rotational correlation time (ϕ_2), which reflects the motion of the entire molecule, was predominant. Furthermore, the amplitude of the local motion of Trp58 was significantly larger than that of Trp22 ($\beta_1^{W58+} > \beta_1^{W22+}$), indicating that local motions of Trp22 are more restricted as compared to Trp58. This is reflected by differences in angular displacements (see eq 4 in the Experimental Procedures) of the two tryptophans within the apoproteins being 16° and 40° for Trp22 and Trp58, respectively. The lower

Table 3: Fluorescence Decay Parameters for the E9 DNase Mutants W22+ and W58+

protein[a]	α_1[b]	α_2	α_3	α_4	τ_1 (ns)	τ_2 (ns)	τ_3 (ns)	τ_4 (ns)	$\langle\tau\rangle$ (ns)	χ^2[c]
W22+		0.156	0.493	0.351		0.96 ± 0.05	3.43 ± 0.12	5.49 ± 0.08	3.77	1.10
W22+−Zn^{2+}		0.280	0.261	0.459		0.87 ± 0.04	2.14 ± 0.11	4.63 ± 0.02	2.93	1.14
W22+−Im9	0.263	0.294	0.181	0.263	0.17 ± 0.01	0.69 ± 0.05	1.71 ± 0.09	4.84 ± 0.01	1.83	1.15
W22+−Zn^{2+}−Im9	0.269	0.365	0.196	0.170	0.14 ± 0.01	0.71 ± 0.03	1.83 ± 0.06	4.71 ± 0.02	1.45	1.20
W58+	0.213	0.156	0.298	0.333	0.02 ± 0.01	0.67 ± 0.03	3.08 ± 0.06	7.71 ± 0.03	3.60	1.06
W58+−Zn^{2+}		0.063	0.161	0.776		0.53 ± 0.08	3.19 ± 0.18	7.67 ± 0.03	6.50	1.01
W58+−Im9	0.234	0.287	0.050	0.429	0.05 ± 0.01	0.33 ± 0.01	2.56 ± 0.20	8.20 ± 0.02	3.75	1.03
W58+−Zn^{2+}−Im9	0.245	0.286	0.052	0.418	0.03 ± 0.01	0.31 ± 0.01	2.31 ± 0.16	8.30 ± 0.01	3.69	1.00

[a] W22+ and W58+ represent the protein E9 DNase containing solely Trp22 or Trp58, respectively, in the absence or presence of zinc (Zn^{2+}). Im9 is representing the immunity protein Im9. [b] α_1, α_2, α_3, and α_4 are the fractional preexponential factors corresponding to lifetimes τ_1, τ_2, τ_3, and τ_4, respectively. [c] Reduced χ^2 values indicate goodness of fit.

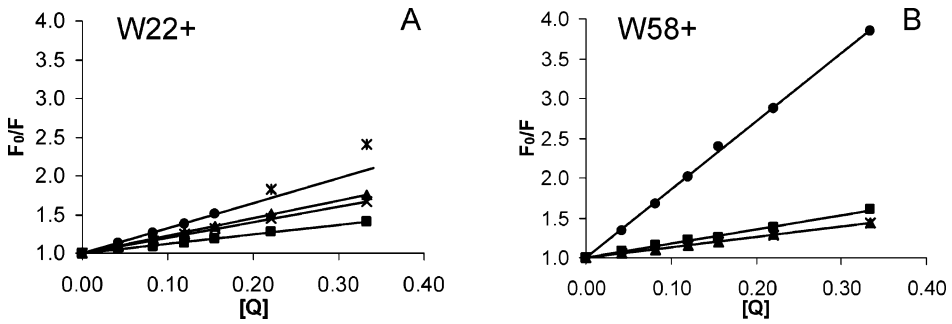

FIGURE 3: Acrylamide quenching of the fluorescence of single Trp mutants. Stern−Volmer plots were obtained from the steady-state fluorescence quenching experiments of E9 DNase mutants W22+ and W58+ shown in panels A and B, respectively. Lines representing the free E9 DNase are shown by (●), in the presence of Zn^{2+} (■), in the presence of immunity protein Im9 (▲), and in the presence of Zn^{2+} and Im9 (×). Before fitting two final data points (*) (indicative of a static component) were omitted.

Table 4: Anisotropy Decay Parameters for the E9 DNase Mutants W22+ and W58+

protein[a]	β_1[b]	β_2	ϕ_1 (ns)	ϕ_2 (ns)	χ^2[c]	ψ[d]
W22+	0.011	0.183	1.39 ± 0.72	11.6 ± 0.3	1.11	16
W22+−Zn^{2+}		0.201		9.4 ± 0.1	1.12	0
W22+−Im9		0.209		18.6 ± 0.2	1.13	0
W22+−Zn^{2+}−Im9		0.203		18.3 ± 0.3	1.22	0
W58+	0.061	0.132	0.68 ± 0.05	11.5 ± 0.2	1.05	40
W58+−Zn^{2+}	0.013	0.208	0.69 ± 0.26	9.7 ± 0.1	1.01	16
W58+−Im9	0.022	0.192	0.83 ± 0.16	17.0 ± 0.2	1.02	22
W58+−Zn^{2+}−Im9	0.024	0.192	0.64 ± 0.12	16.6 ± 0.2	1.03	22

[a] W22+ and W58+ represent the protein E9 DNase containing solely Trp22 or Trp58, respectively, in the absence or presence of zinc (Zn^{2+}). Im9 represents the immunity protein Im9. [b] β_1 and β_2 are the amplitudes corresponding to the rotational correlation times ϕ_1 and ϕ_2, respectively. [c] Reduced χ^2 values indicate goodness of fit. [d] ψ is the angular displacement (in degrees) of the fluorophore.

Table 5: Summary of Fluorescence Quenching Studies with Acrylamide

protein[a]	K_{SV} (M^{-1})[b]	k_q (ns^{-1} M^{-1})
W22+	3.28 ± 0.26[c]	1.11
W22+−Zn^{2+}	1.22 ± 0.03	0.42
W22+−Im9	2.26 ± 0.03	1.23
W22+−Zn^{2+}−Im9	2.01 ± 0.02	1.38
W58+	8.63 ± 0.07	2.40
W58+−Zn^{2+}	1.80 ± 0.06	0.28
W58+−Im9	1.33 ± 0.02	0.35
W58+−Zn^{2+}−Im9	1.33 ± 0.02	0.36

[a] W22+ and W58+ represent the protein E9 DNase containing Trp22 and Trp58, respectively, in the absence or presence of zinc (Zn^{2+}). Im9 represents the immunity protein Im9. [b] K_{SV} values were determined via Stern−Volmer analysis (see Experimental Procedures, eq 5). [c] Before fitting, the two final data points (indicative of a static component) were omitted (see also Figure 3A).

value for the short rotational time (ϕ_1) for W58+ indicates that, in addition to a larger angular freedom, Trp58 moves faster than Trp22.

Binding of Zn^{2+} to either W22+ or W58+ (Table 4) resulted in a reduction of the long rotational correlation time (ϕ_2) in both the Im9-free and Im9-bound forms, consistent with the effects on the wild-type protein (Table 2). Moreover, Zn^{2+} binding as well as Im9 binding had a marked effect on the local mobility (ϕ_1) of both Trp22 and Trp58. Binding of either Zn^{2+} or Im9 (or both) to W22+ eliminated ϕ_1, indicating that Trp22 was immobilized within the protein. While binding either ligand did not eliminate the shorter correlation time in W58+ (Table 4), it did reduce its contribution (β_1) substantially. Hence, while the rate of rotation had not decreased, the angular displacement of Trp58 was reduced from 40° to 16° and 22° upon Zn^{2+} and Im9 binding, respectively. As compared with the binary W58+−Im9 complex, the angular displacement of Trp58 was the same for W58+−Zn^{2+}−Im9. Moreover, the differences in the short correlation time (ϕ_1) are not significantly distinct (binary complex 0.8 ± 0.2 vs ternary complex 0.6 ± 0.1). This was confirmed by global analysis of both data sets: when the individual anisotropy decays of W58+−Im9 and W58+−Zn^{2+}−Im9 were forced to be the same, the overall χ^2 remained small (1.13).

Steady-State Fluorescence Quenching Studies of the E9 DNase Mutants. The solvent accessibility of the tryptophans in the E9 DNase variants was probed by acrylamide quenching experiments. The resulting Stern−Volmer plots and constants are shown in Figure 3 and listed in Table 5, respectively. Upon Zn^{2+} binding (Table 5), both the W22+ mutant and the W58+ mutant showed a clear decrease in collisional encounters between the fluorophore and acrylamide. This indicates that both tryptophans experience solvent protection. However, the protection provided by Zn^{2+} was more pronounced for Trp58 than for Trp22. In contrast, Im9 affected the two protein differently: Im9 binding to W22+ did not significantly affect the rate of collisional encounters, whereas it reduced it by ~7-fold for W58+ (see Table 5 and Figure 3). This indicates that the solvent accessibility of Trp22 was largely unaffected by Im9 binding, whereas for Trp58 it decreased dramatically. The presence of Zn^{2+} in the ternary E9−Zn^{2+}−Im9 complexes had no substantial effect, in agreement with the dominant effect of Im9 binding described above.

DISCUSSION

In the present work we have used time-resolved fluorescence and anisotropy to analyze how binding of two inhibitors of DNase activity affected the conformational dynamics of colicin E9 DNase on the nanosecond time scale. We focused on the E9 DNase, as it is the best characterized of the four colicin DNases (E2, E7, E8, and E9). The two inhibitors were chosen because they bind at different sites on the protein (the active site and an exosite, respectively) and inhibit the enzyme by different mechanisms (chelation of catalytic residues and steric electronic exclusion, respectively).

Ligand-Induced Conformational Changes: Zinc. While the average fluorescence lifetime for both W22+ and W58+

DNases is affected upon Zn^{2+} binding, the manner by which it occurs differs markedly. The decrease in average lifetime for W22+ implies that upon Zn^{2+} binding the indole side chain of Trp22 (located in the short helix II, length ~9 Å) interacts to a greater extent with neighboring groups within E9 DNase. This effect is accompanied by a decrease in its solvent exposure (Figure 3A) and the disappearance of its rotational freedom (Table 4), all pointing to an increased compactness of the E9 DNase in the Zn^{2+}-bound form, an effect that we have previously observed by ESI-MS (*19*). This increased compactness of the E9 DNase also affects Trp58 (located in helix IV, length ~21 Å), resulting in a decreased solvent accessibility (Figure 3B) and rotational freedom ψ drops (from 40° to 16°, Table 4). This increased compactness is likely to be the origin of the increased average lifetime for Trp58 that occurs due to the disappearance of the subnanosecond lifetime component τ_1 (0.21 ns) and a decrease in the contribution of τ_2 (~0.50 ns). Subnanosecond lifetimes are interpreted as the result of excited-state quenching of tryptophan emission by the protein backbone (*33*). Apparently, in the Zn^{2+}-ligated compact state the E9 DNase adopts a conformation that prohibits interaction between Trp58 and the protein backbone. The remaining lifetime components τ_3 (3.1 ns) and τ_4 (7.7 ns) are typical decay times for the tryptophan's indole moiety in environments of different polarity, and these were unaffected upon Zn^{2+} binding.

Crystal structures of the E9 DNase in different metal ion occupancies demonstrate that, in the crystal state, Zn^{2+} binding to E9 DNase induces conformational changes that involve rearrangements of hydrogen-bonding patterns as well as movement of the C-terminal α-helix to produce a closure of the active site and a more compact structure (*22*, *34*, *35*). Recently, we showed by ESI-MS that compaction of colicin DNase on Zn^{2+} binding also occurs in the solution state (*19*, *20*). The decrease in the long rotational correlation time (Table 4) confirms these observations.

Although the two tryptophans of the E9 DNase are 13−15 Å from the position of the metal ion, Trp58 is at the base of the active site cleft and is significantly more solvent exposed, as indicated by the fluorescence emission maximum of 338 nm for W58+ compared to 333 nm for W22+ (*12*). Accordingly, Zn^{2+} binding closes the active site protecting Trp58, sitting at its base, from acrylamide. Whereas both NMR and crystallography indicate that closure of the E9 DNase structure is structurally localized to the active site (*21*, *22*), our ESI-MS experiments (*19*, *20*) demonstrate that binding of Zn^{2+} does have a greater impact on the global structure of the protein in solution. These findings correlate with the present results where the environment of Trp22 is affected in addition to that of Trp58. To account for this "globally transmitted" effect, we suggest that closure of the active site upon Zn^{2+} binding occurs like a clasp closing with the pivot point located near to Trp22. This would explain why relatively small structural changes close to Trp22 have a disproportionally large effect on its mobility at the nanosecond time scale, which are not detected by NMR (*21*). Moreover, such a clasp closure mechanism is in good agreement with our ESI-MS experiments (*19*, *20*).

Ligand-Induced Conformational Changes: Im9. The ultrashort lifetime of Im9 alone is most likely due to hydrogen bonding between Trp74 and His46, which covers most of the indole side chain. This interaction is likely the reason Im9 is immobile on the (sub)nanosecond time scale. No additional rotational correlation times appear on Im9 binding to E9 DNase. These observations are consistent with previous structural data, which shows only very minor conformational changes for Im9 on complexation with E9 DNase (*36*). Since both the single tryptophan of Im9 and the tryptophans within E9 DNase have multiple lifetime components, caution must be taken when analyzing the effects of Im9 binding on the lifetimes of Trp22 and Trp58. Hence, on the basis of fluorescence lifetime analysis firm conclusions are not easy to draw about the effect of Im9 binding on the conformational dynamics of E9. The availability of a Trp-free Im9 mutant would circumvent this problem. However, constructing a mutant representative of native Im9 is cumbersome because the hydrogen bond between Trp74 and His46 is crucial for the conformational stability of Im9 (*37*). Still, since the amplitudes (α values) of the longer fluorescence lifetimes for Trp22 and Trp58 in the free E9 DNase are much greater than that of free Im9, they should dominate within the E9−Im9 complex if no structural changes would occur on complexation. Of particular interest is the effect of Im9 binding on the longest lifetime component (τ_4) of Trp22 and Trp58, which shows a small decrease (from 5.5 to 4.8 ns, Table 3) or increase (from 7.7 to 8.2 ns), respectively. The decrease for Trp22 indicates an increase in the interaction with neighboring groups within E9 DNase, which results in the loss of the short rotational correlation time (ϕ_1) and a decreased solvent accessibility. Furthermore, the observed decrease in angular displacement of Trp58 (Table 4) indicates restricted mobility on Im9 binding.

Analogous to Zn^{2+} binding, complexation of E9 DNase with Im9 leads to structural changes that are transmitted through the protein from the binding site for the immunity protein to the tryptophans, which are both away from the binding site. One of the regions of the E9 DNase affected by the mobility of Trp22 on the seconds time scale spans residues 67−72, with the immunity protein binding site extending from residues 72 to 99 (*6*, *18*). Boetzel et al. (*36*) proposed that ligation of Asn72 of the E9 DNase to Im9 could explain the effects of Im9 binding on Trp22. However, the fluorescence changes accompanying Im9 binding to the wild-type E9 DNase have also been observed for the E9 DNase N72A mutant (A. H. Keeble and C. Kleanthous, unpublished observations). Instead, interactions of Im9 with the main chain of the DNase within the immunity protein binding site are the likely origin of the alteration in Trp22 as transmitted by the 67−72 region of the DNase. For Trp58, binding effects are possibly transmitted through Pro85, which is the neighboring residue of Phe86 that is critical for the interaction with Im9, with the ring of Pro85 coming within van der Waals distance (3.55−3.76 Å) from the indole ring of Trp58 (*6*, *22*). However, comparison of the crystal structures of the immunity protein bound form and free DNase does not help since the positions of the side chains within the DNase in both structures are essentially identical (*35*). The present work demonstrates that the structural changes induced by Im9 binding clearly affect both tryptophans, rather than only Trp22 as is implied by the proposed immunity protein binding mechanisms (*17*, *18*).

Im9-Induced Conformational Changes Occur Independently of Zn^{2+}-Induced Conformational Effects. Although

Zn^{2+} binding affects the DNase tryptophan environment within the E9−Im9 binary complex (solely for Trp22), the extent of the effect is much less than for binding to the free E9 DNase, indicating that Im9-induced conformational changes have primacy over those induced by Zn^{2+} binding. This observation agrees well with the stopped-flow fluorescence experiments of Keeble et al. (*12*), which demonstrated that the kinetics of immunity protein binding to E9 DNase are essentially identical with or without bound metal ion, indicating that the bound metal ion does not affect the kinetics of Im9 binding. The present work also has important consequences for the mechanism of cell entry by colicin E9 proposed by Pommer et al. (*16*). They suggested that removal of the bound metal ion destabilizes the high-affinity colicin DNase−immunity protein complex [K_d, $\sim 10^{-14}$ M (*15*)], thereby accelerating the dissociation rate so that it is not rate limiting for toxin-induced cell death. The present experiments discount this possibility, and therefore, some other factor must be involved in enhancing the dissociation rate of the E9−Im9 complex at the cell surface.

Colicin DNases Highlight Distinct Conformational Equilibria. In the present work we have used a combination of time-resolved anisotropy and time-resolved fluorescence decays to investigate the conformational dynamics within colicin DNase domains. This represents the first analysis of the conformational dynamics of colicin DNases on the nanosecond time scale. The demonstration that *both* tryptophans are rotationally mobile relative to the protein is a feature that is not observed by either crystallography or NMR and illustrates the usefulness of the present techniques in fully understanding the conformational dynamics of the colicin DNases. Moreover, time-resolved fluorescence decay experiments demonstrated that the presence of multiple fluorescence lifetimes in the wild-type E9 DNase is due to both Trp22 and Trp58. Many proteins containing only a single tryptophan exhibit multiple fluorescence lifetimes (*29*). This is due to the tryptophans experiencing different microenvironments within the protein and is thus a response to the presence of conformational dynamics within the protein. We have previously characterized two "forms" of conformational dynamics that are present within colicin DNases. The first one represents an equilibrium between an open and closed conformation, as detected by ESI-MS, that is biased toward the open form for the E7 DNase and toward the closed form for the E8 DNase and intermediate for E2 and E9 DNase (*19*, *20*). The second form represents a type of conformational heterogeneity centered around Trp22, as detected by high-field NMR experiments, and affects residues within a 9 Å radius (*17*). However, the present time-resolved fluorescence and anisotropy results are inconsistent with these equilibria being the origin of the dynamics probed by tryptophan fluorescence measurements. Two examples illustrate this point. First, the fluorescence lifetime and rotational correlation times are rather similar for the different wild-type colicin DNases (*20*; E. T. J. van den Bremer and A. J. R. Heck, unpublished results), despite the observed differences between the open−closed equilibria. Second, the fluorescence decays are markedly affected upon Zn^{2+} binding, whereas NMR experiments showed no changes in the dynamics of the tryptophans occurring upon Zn^{2+} binding (*21*). Kinetic investigations of ligand binding to the colicin DNases (*12*) have also provided evidence for the independence of these processes from those that affect the tryptophans upon ligand binding. Furthermore, we have previously demonstrated that the conformational equilibria detected by ESI-MS are independent of those probed by NMR (*19*). However, a more fundamental reason underpins why the conformational dynamics detected in the present study are not a result of the dynamic processes monitored by NMR and ESI-MS that occur over much longer time scales. Whereas the processes probed by the present time-resolved experiments occur on the nanosecond time scale, the open−closed equilibrium detected by ESI-MS is likely to take place over microseconds to seconds (typical time scales for folding/unfolding events), while the NMR detects conformational heterogeneity occurring on the second time scale. Furthermore, the relative commonality of multiple fluorescence decays in single-tryptophan-containing proteins itself argues that it is a fundamental dynamic property of the tryptophans rather than a side effect of another process. However, it remains possible that these other conformational equilibria may *influence* the magnitudes of the fluorescence decay lifetimes if the microenvironments of the tryptophans are different between the conformers, with the observed values being determined by the equilibrium contribution of each conformer.

In conclusion, using time-resolved tryptophan fluorescence and anisotropy, we have shown how binding of two inhibitors of DNase activity, Zn^{2+} and Im9, influences in a distinct manner the conformational dynamics of the DNase colicin E9. One feature both inhibitors share is that these conformational differences are transmitted throughout the DNase protein from the metal binding site or from the immunity protein exosite to both tryptophans, which in this respect has not been detected with other techniques for colicin DNases so far. Moreover, the results of this study indicate that Im9-induced conformational effects predominate over Zn^{2+}-induced effects.

REFERENCES

1. James, R., Penfold, C. N., Moore, G. R., and Kleanthous, C. (2002) Killing of *E. coli* cells by E group nuclease colicins, *Biochimie 84*, 381−389.
2. Pommer, A. J., Cal, S., Keeble, A. H., Walker, D., Evens, S. J., Kuhlman, U. C., Cooper, A., Connolly, B. A., Hemmings, A. M., Moore, G. R., James, R., and Kleanthous, C. (2001) Mechanisms and cleavage specificity of the H-N-H endonuclease colicin E9, *J. Mol. Biol. 314*, 735−749.
3. Walker, D. C., Georgiou, T., Pommer, A. J., Walker, D., Moore, G. R., Kleanthous, C., and James, R. (2002) Mutagenic scan of the H-N-H motif of colicin E9: implications for the mechanistic enzymology of colicins, homing enzymes and apoptotic endonucleases, *Nucleic Acids Res. 30*, 3225−3234.
4. Taylor, R., Burgner, J. W., Clifton, J., and Cramer, W. A. (1998) Purification and characterization of monomeric *Escherichia coli* vitamin B12 receptor with high affinity for colicin E3, *J. Biol. Chem. 273*, 31113−31118.
5. Di Masi, D. R., White, J. C., Schnaitman, C. A., and Bradbeer, C. (1973) Transport of vitamin B12 in *Escherichia coli*: common receptor sites for vitamin B12 and the E colicins on the outer membrane of the cell envelope, *J. Bacteriol. 115*, 506−513.
6. Kleanthous, C., Kuhlmann, U. C., Pommer, A. J., Ferguson, N., Radford, S. E., Moore, G. R., James, R., and Hemmings, A. M. (1999) Structural and mechanistic basis of immunity toward endonuclease colicins, *Nat. Struct. Biol. 6*, 243−252.
7. Buckle, A. M., and Fersht, A. R. (1994) Subsite binding in an RNase: structure of a barnase-tetranucleotide complex at 1.76-A resolution, *Biochemistry 33*, 1644−1653.

8. Kleanthous, C., and Walker, D. (2001) Immunity proteins: enzyme inhibitors that avoid the active site, *Trends Biochem. Sci. 26*, 624−631.
9. Galburt, E. A., and Stoddard, B. L. (2002) Catalytic mechanisms of restriction and homing endonucleases, *Biochemistry 41*, 13851−13860.
10. Kuhlmann, U. C., Moore, G. R., James, R., Kleanthous, C., and Hemmings, A. M. (1999) Structural parsimony in endonuclease active sites: should the number of homing endonuclease families be redefined?, *FEBS Lett. 463*, 1−2.
11. Scholz, S. R., Korn, C., Bujnicki, J. M., Gimadutdinow, O., Pingoud, A., and Meiss, G. (2003) Experimental Evidence for a $\beta\beta\alpha$-Me-Finger Nuclease Motif To Represent the Active Site of the Caspase-Activated DNase, *Biochemistry 42*, 9288−9294.
12. Keeble, A. H., Hemmings, A. M., James, R., Moore, G. R., and Kleanthous, C. (2002) Multistep Binding of Transition Metals to the H-N-H Endonuclease Toxin Colicin E9, *Biochemistry 41*, 10234−10244.
13. Sui, M. J., Tsai, L. C., Hsia, K. C., Doudeva, L. G., Ku, W. Y., Han, G. W., and Yuan, H. S. (2002) Metal ions and phosphate binding in the H-N-H motif: crystal structures of the nuclease domain of ColE7/Im7 in complex with a phosphate ion and different divalent metal ions, *Protein Sci. 11*, 2947−2957.
14. Wallis, R., Leung, K. Y., Pommer, A. J., Videler, H., Moore, G. R., James, R., and Kleanthous, C. (1995) Protein−protein interactions in colicin E9 DNase−immunity protein complexes. 2. Cognate and noncognate interactions that span the millimolar to femtomolar affinity range, *Biochemistry 34*, 13751−13759.
15. Wallis, R., Moore, G. R., James, R., and Kleanthous, C. (1995) Protein−protein interactions in colicin E9 DNase−immunity protein complexes. 1. Diffusion-controlled association and femtomolar binding for the cognate complex, *Biochemistry 34*, 13743−13750.
16. Pommer, A. J., Kuhlmann, U. C., Cooper, A., Hemmings, A. M., Moore, G. R., James, R., and Kleanthous, C. (1999) Homing in on the role of transition metals in the HNH motif of colicin endonucleases, *J. Biol. Chem. 274*, 27153−27160.
17. Whittaker, S. B., Boetzel, R., MacDonald, C., Lian, L. Y., Pommer, A. J., Reilly, A., James, R., Kleanthous, C., and Moore, G. R. (1998) NMR detection of slow conformational dynamics in an endonuclease toxin, *J. Biomol. NMR 12*, 145−159.
18. Whittaker, S. B., Czisch, M., Wechselberger, R., Kaptein, R., Hemmings, A. M., James, R., Kleanthous, C., and Moore, G. R. (2000) Slow conformational dynamics of an endonuclease persist in its complex with its natural protein inhibitor, *Protein Sci. 9*, 713−720.
19. Van den Bremer, E. T. J., Jiskoot, W., James, R., Moore, G. R., Kleanthous, C., Heck, A. J. R., and Maier, C. S. (2002) Probing metal ion binding and conformational properties of the colicin E9 endonuclease by electrospray ionization time-of-flight mass spectrometry, *Protein Sci. 11*, 1738−1752.
20. Van den Bremer, E. T. J., Keeble, A. H., Jiskoot, W., Spelbrink, R. E. J., Maier, C. S., Van Hoek, A., Visser, A. J. W. G., James, R., Moore, G. R., Kleanthous, C., and Heck, A. J. R. (2004) Distinct conformational stability and functional activity of four highly homologous endonuclease colicins, *Protein Sci.* (in press).
21. Hannan, J. P., Whittaker, S. B., Hemmings, A. M., James, R., Kleanthous, C., and Moore, G. R. (2000) NMR studies of metal ion binding to the Zn-finger-like HNH motif of colicin E9, *J. Inorg. Biochem. 79*, 365−370.
22. Kuhlmann, U. C., Pommer, A. J., Moore, G. R., James, R., and Kleanthous, C. (2000) Specificity in protein−protein interactions: the structural basis for dual recognition in endonuclease colicin-immunity protein complexes, *J. Mol. Biol. 301*, 1163−1178.
23. Garinot-Schneider, C., Pommer, A. J., Moore, G. R., Kleanthous, C., and James, R. (1996) Identification of putative active-site residues in the DNase domain of colicin E9 by random mutagenesis, *J. Mol. Biol. 260*, 731−742.
24. Vos, K., Van Hoek, A., and Visser, A. J. W. G. (1987) Application of a reference convolution method to tryptophan fluorescence in proteins. A refined description of rotational dynamics, *Eur. J. Biochem. 165*, 55−63.
25. Van Hoek, A., and Visser, A. J. W. G. (1985) Artefact and distortion sources in time correlated single photon counting, *Anal. Instrum. 14*, 359−378.
26. Digris, A. V., Skakun, V. V., Novikov, E. G., Van Hoek, A., Claiborne, A., and Visser, A. J. W. G. (1999) Thermal stability of a flavoprotein assessed from associative analysis of polarized time-resolved fluorescence spectroscopy, *Eur. Biophys. J. 28*, 526−531.
27. Novikov, E. G., Van Hoek, A., Visser, A. J. W. G., and Hofstraat, J. W. (1999) Linear algoritms for stretched exponential decay analysis, *Opt. Commun. 166*, 189−198.
28. Szabo, A. (1984) Theory of fluorescence depolarization in macromolecules and membranes, *J. Chem. Phys. 81*, 150−167.
29. Lakowicz, J. R. (1999) *Principles of Fluorescence Spectroscopy*, 2nd ed., Kluwer Academic/Plenum Publishers, New York, Dordrecht, London, and Moscow.
30. Malnasi-Csizmadia, A., Woolley, R. J., and Bagshaw, C. R. (2000) Resolution of conformational states of Dictyostelium myosin II motor domain using tryptophan (W501) mutants: implications for the open-closed transition identified by crystallography, *Biochemistry 39*, 16135−16146.
31. Moncrieffe, M. C., Venyaminov, S. Y., Miller, T. E., Guzman, G., Potter, J. D., and Prendergast, F. G. (1999) Optical spectroscopic characterization of single tryptophan mutants of chicken skeletal troponin C: evidence for interdomain interaction, *Biochemistry 38*, 11973−11983.
32. Azuaga, A. I., Canet, D., Smeenk, G., Berends, R., Titgemeijer, F., Duurkens, R., Mateo, P. L., Scheek, R. M., Robillard, G. T., Dobson, C. M., and van Nuland, N. A. (2003) Characterization of single-tryptophan mutants of histidine-containing phosphocarrier protein: evidence for local rearrangements during folding from high concentrations of denaturant, *Biochemistry 42*, 4883−4895.
33. Kungl, A. J., Visser, N. V., van Hoek, A., Visser, A. J. W. G., Billich, A., Schilk, A., Gstach, H., and Auer, M. (1998) Time-resolved fluorescence anisotropy of HIV-1 protease inhibitor complexes correlates with inhibitory activity, *Biochemistry 37*, 2778−2786.
34. Ko, T. P., Liao, C. C., Ku, W. Y., Chak, K. F., and Yuan, H. S. (1999) The crystal structure of the DNase domain of colicin E7 in complex with its inhibitor Im7 protein, *Struct. Folding Des. 7*, 91−102.
35. Kolade, O. O., Carr, S. B., Kuhlmann, U. C., Pommer, A., Kleanthous, C., Bouchcinsky, C. A., and Hemmings, A. M. (2002) Structural aspects of the inhibition of DNase and rRNase colicins by their immunity proteins, *Biochimie 84*, 439−446.
36. Boetzel, R., Czisch, M., Kaptein, R., Hemmings, A. M., James, R., Kleanthous, C., and Moore, G. R. (2000) NMR investigation of the interaction of the inhibitor protein Im9 with its partner DNase, *Protein Sci. 9*, 1709−1718.
37. Wallis, R., Leung, K. Y., Osborne, M. J., James, R., Moore, G. R., and Kleanthous, C. (1998) Specificity in protein−protein recognition: conserved Im9 residues are the major determinants of stability in the colicin E9 DNase−Im9 complex, *Biochemistry 37*, 476−485.

BI049929C